Online-Journals.org

iJOE International Journal of Online and Biomedical Engineering

iJOE | eISSN: 2626-8493 | Vol. 21 No. 8 (2025) | OPEN ACCESS

https://doi.org/10.3991/ijoe.v21i08.54583

PAPER

# Enhancing Digital Healthcare through 5G Integration Using a Slotted Bow-Tie 4 × 1 Patch Antenna Array

**Zribi Chedly[1], Beldi Sabri[1], Azizi Mohamed Karim[1,2], Amor Smida[1,3], Naif Hadeed Al-Mutairi[4], Mohamed Ibrahim Waly[3](✉)**

[1]Microwave Electronics Research Laboratory, Faculty of Sciences of Tunis, University of Tunis El Manar, Tunis, Tunisia

[2]Higher Institute of Arts Mulimedia of Manouba, University of Manouba, Manouba, Tunisia

[3]Department of Medical Equipment Technology, College of Applied Medical Sciences, Majmaah University, Al-Majmaah, Saudi Arabia

[4]King Khalid Hospital in Al Majmaah, Ministry of Health, Riyadh Second Health Cluster, Riyadh, Saudi Arabia

m.waly@mu.edu.sa

**ABSTRACT**

This paper explores the transformative potential of integrating fifth generation (5G) mobile communication technology into digital healthcare. The advanced features of 5G, such as high data speed, minimal delay, and extensive device connectivity, can enhance healthcare applications, including remote surgeries, teleconsultations, wearable device applications, and big data management. A novel high return loss and high gain slots Bow-Tie microstrip patch antenna array for 5G applications is proposed to support this integration. The antenna design process, simulations, and measurements are detailed, highlighting the antenna's performance at a frequency of 5.8 GHz. The study concludes that the synergistic combination of 5G technology and the proposed antenna design can significantly improve digital healthcare delivery.

**KEYWORDS**

healthcare, fifth generation (5G) applications, microstrip Bow-Tie antenna, slots, 4 × 1 Bow-Tie antenna array

## 1 INTRODUCTION

The integration of fifth generation (5G) mobile communication technology into digital healthcare offers the potential to revolutionize healthcare delivery by enabling high-speed data transmission, ultra-low latency, massive device connectivity, and increased network capacity. These features support a range of healthcare applications, including remote robotic surgery, teleconsultations, in-ambulance treatment, and wearable devices within the Internet of Things (IoT) framework [1–5]. Effective deployment of 5G in healthcare requires a deep understanding of communication needs, allowing stakeholders to select appropriate wireless technologies and ensure seamless integration into healthcare systems [6, 7].

5G's low latency and high bandwidth are key to advancing healthcare applications such as remote surgeries and in-ambulance treatments, driving the design, deployment, and evaluation of systems that meet these needs [4]. Understanding these

Chedly, Z., Sabri, B., Karim, A.M., Smida, A., Al-Mutairi, N.H., Waly, M.I. (2025). Enhancing Digital Healthcare through 5G Integration Using a Slotted Bow-Tie 4 × 1 Patch Antenna Array. *International Journal of Online and Biomedical Engineering (iJOE)*, 21(8), pp. 138–154. https://doi.org/10.3991/ijoe.v21i08.54583

Article submitted 2025-01-23. Revision uploaded 2025-03-18. Final acceptance 2025-03-18.

communication requirements ensures that healthcare systems function optimally with 5G technology. A critical element in this integration is the deployment of advanced antenna technologies, such as the Slotted Bow-Tie 4 × 1 patch antenna array, which enhances 5G connectivity and addresses the diverse needs of modern healthcare applications.

The integration of 5G technology into healthcare faces challenges such as interference with medical devices, the feasibility of large-scale telemedicine deployment, and the integration of IoT healthcare applications. Hospitals need to manage electromagnetic interference (EMI) and ensure reliable coverage using small-cell networks and careful antenna placement [8]. Deploying 5G in rural areas for telemedicine is hindered by infrastructure costs, while wearable healthcare devices require miniaturized, energy-efficient antennas [9]. The Slotted Bow-Tie antenna offers potential solutions in this area, but miniaturization remains a challenge. Furthermore, as IoT devices in healthcare generate vast amounts of data, the 5G network must support massive device connectivity and low-latency communication, which requires efficient network management, prioritization, and data security protocols to protect sensitive patient information [10–11]. Addressing these challenges will require collaboration between technology developers, healthcare providers, and regulatory authorities.

The growing demand for higher capacity and faster data rates in telecommunications is being addressed by 5G technology, with promises of supporting up to 1000 times the capacity of current networks by 2030 [12, 13]. This evolution has spurred innovations in broadband antenna technology, which is vital for enabling seamless and high-speed data transmission in digital healthcare systems. The small cell architecture of 5G networks enhances coverage and capacity, supporting various applications and services, including those in healthcare [14].

The Bow-Tie antenna, first proposed in 1996 by J. George [15], has proven versatile in applications such as ground-penetrating radar and wireless communications [16–18]. Its wide operating bandwidth, higher gain, and low cross-polarization levels make it an ideal choice for digital healthcare applications, especially in miniaturized and compact designs [19–23]. Recent advancements in Bow-Tie antennas have led to better performance, offering solutions for 5G communication needs [24–26].

Studies highlight the potential of antennas for biomedical and communication applications, with Alsaraira et al. [27] demonstrating UWB antennas' role in diagnostic systems, Zhang et al. [28] emphasizing compact designs for portable devices, and Kumar and Singh [29] optimizing antenna arrays for 5G communication. Building on these insights, this study integrates a slotted Bow-Tie structure into a 4 × 1 patch antenna array to enhance digital healthcare systems operating in 5G environments. The design focuses on bridging theoretical advancements with practical applications, promising improved performance in healthcare communication.

## 2 MATERIAL AND METHODOLOGY

### 2.1 Single Bow-Tie antenna design

A Bow-Tie Patch antenna design (see Figure 1) was chosen due to its ability to conform to the suit, along with its large gain and wideband characteristics. The microstrip Bow-Tie patch antenna with slots is shown in Figure 1. Here, L is the

substrate length, W is the substrate width, D is the feed width, Hb is the side length of the Bow-Tie, and Wb is the side width of the Bow-Tie, respectively. The first two slots have the shape of two equilateral triangles placed on each patch, with Ht = 4 mm as the side length of the triangle. The second slot is a rectangle with a width of Ws = 8 mm and a length of Ls = 1 mm. The Bow-Tie Patch antenna has been designed to operate at 5.8 GHz.

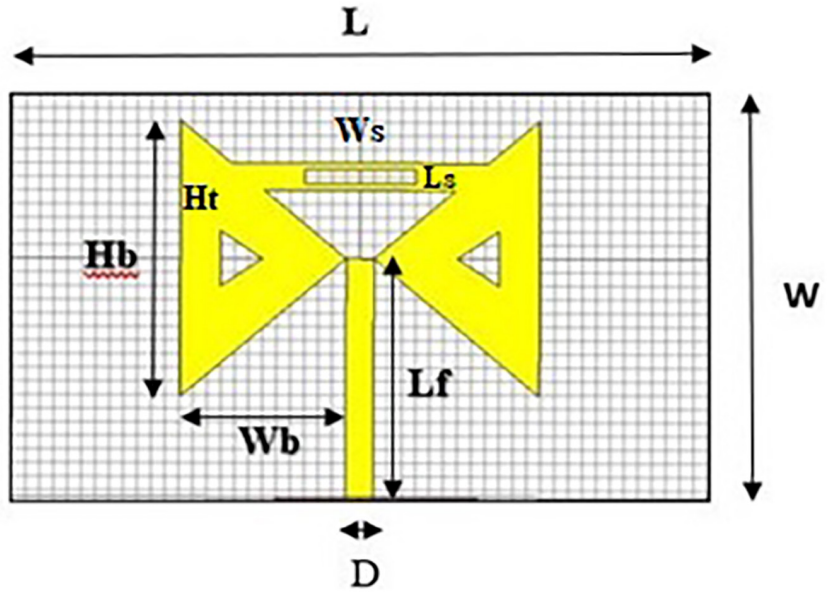


**Fig. 1.** Geometry of the proposed Bow-Tie Patch antenna with slots, showing key dimensions (L, W, D, Hb, Wb, Ht, Wt, Ls, and Lf)

FR4 is defined by its mechanical properties, such as its permittivity ($\varepsilon_r = 4.3$) and its thickness of 1.6 mm. A 50 Ω waveguide port is used to feed power into the radiator. To design single Bow-Tie antenna, precise formulas or equations are used to calculate the antenna dimensions:

**a)** Calculation of Lambda: (λ)

$$\lambda = c/f \quad (1)\ [30]$$
$$\lambda = 54 \text{ mm}$$

**b)** Calculation of the side width of Bow Tie: (Wb)
The side width Wb is given as:

$$Wb = \lambda/(2*\text{sqrt}(\varepsilon\_r)) \quad (2)\ [31]$$
$$Wb = 54/2*\text{sqrt}(4.4) = 54/2.19$$
$$Wb = 12.8 \text{ mm}$$

Wb = side width, λ = wavelength in free space, ε_r = dielectric constant of material.

**c)** Calculation of Feed line width: (D)

$$Z = 377/(D/h- \text{sqrt}(\varepsilon\_r)) \quad (3)\ [32]$$
$$Z = 377/(D/h- 2.07)$$

D = width of feed line, h = thickness of substrate = 1.6 mm, Feed width (D) = 2 mm

**d)** Calculation of Feed line length: (Lf):

$$Lf = \lambda/(4*\text{sqrt}(\varepsilon\_r)) \quad (4)\ [33]$$
$$Lf = 25\ \text{mm}$$

Table 1 shows a summary of the dimensions for the single Bow-Tie Patch antenna design according to its main components, which include substrate width, substrate length, substrate thickness, side width, side height, feed line width, and feed line length.

**Table 1.** Dimension of single Bow-Tie Patch antenna design

| Part | Symbol | Dimensions |
|---|---|---|
| Substrate width | W | 30 |
| Substrate length | L | 50 |
| Substrate thickness | h | 1.6 |
| Side width | Wb | 12.8 |
| Side height | Hb | 19.4 |
| Feed line width | D | 2 |
| Feed line length | Lf | 25 |

## 2.2 Bowtie 4 × 1 Patch antenna array

The single microstrip Bow-Tie antenna used was designed to enhance gain, bandwidth, and return loss. However, the measurement results were not as good as expected. A solution to achieve resonance at 5.8 GHz with improved return loss and gain is to use a 4 × 1 array structure of the single Bow-Tie antenna. This structure consists of four antennas connected and arranged in a straight line, forming a linear antenna array that functions as a single antenna capable of transmitting or receiving electromagnetic waves more effectively than individual antennas. These individual antennas are interconnected, allowing the signal from one antenna to be transferred to another, thereby creating a more efficient system than a single antenna alone.

All four antennas that make up the antenna array are fed by a single feeder. When placing individual antennas in an array, the spacing between the Bow-Tie antennas should be precise and in exact phase. This ensures that every antenna in a similar direction contributes to the summed radiation beam while signals in other directions are canceled. In this case, the spacing between the four Bow-Tie antennas is considered as λ/4.

This type of arrangement enhances the system's directivity and addresses the issues caused by a single Bow-Tie antenna, such as low gain and high return loss, achieving the desired enhancement. An antenna array also enables the achievement of a maximum SNR ratio, optimizing performance with minimal power wastage while significantly improving signal strength, range, and quality.

It can be noted that, to a great extent, minor lobes are reduced when using the antenna array instead of a single antenna.

To set up this system, the same dimensions of the single Bow-Tie Patch antenna are used:

- The side width of Bow Tie Wb = 12.8 mm.
- Feed line length, Lf = 25 mm.
- Feed line Width D = 2 mm.

The distance taken between two Bow-Tie patches d is λ/2 = 26 mm.

The design of Bow-Tie 4 × 1 Patch antenna array with distance (d) between the elements is depicted in Figure 2.

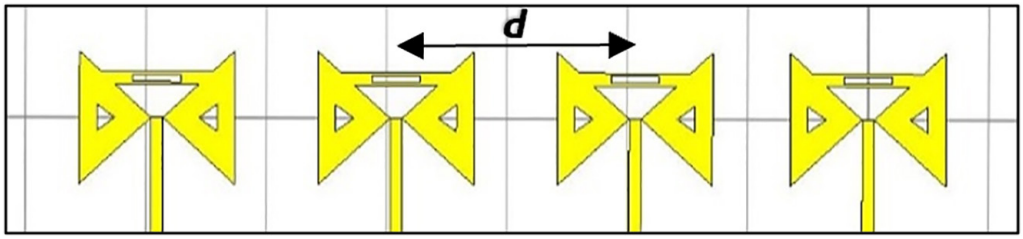


**Fig. 2.** Geometry of the Bow-Tie 4 × 1 Patch antenna array design, with spacing denoted by 'd' between elements

The proposed Bow-Tie antenna is highly scalable and adaptable for various 5G frequency bands and medical device applications. It can be tuned for sub-6 GHz and mm wave frequencies by adjusting its dimensions, with the option to expand into larger arrays for higher gains. The antenna design is suitable for wearable devices, where it can be printed on flexible substrates for conformal body placement, though adjustments may be needed for body loading effects. For implantable devices, miniaturization and biocompatibility are essential, with potential adaptations for lower frequencies to improve tissue penetration. The antenna's compact size also makes it ideal for integration into handheld or body-worn sensors, ensuring versatility in 5G medical applications.

## 3 RESULTS AND DISCUSSIONS

The proposed Bow-Tie Microstrip antenna results are obtained using CST Microwave Studio. In Figure 3, the return loss characteristic of the microstrip Bow-Tie antenna is presented. This simulation shows a resonance frequency at 5.8 GHz with a return loss of –34.45 dB. The gain of the antenna, shown in Figure 4, is approximately 1.21 dB, which is not very high and requires improvement.

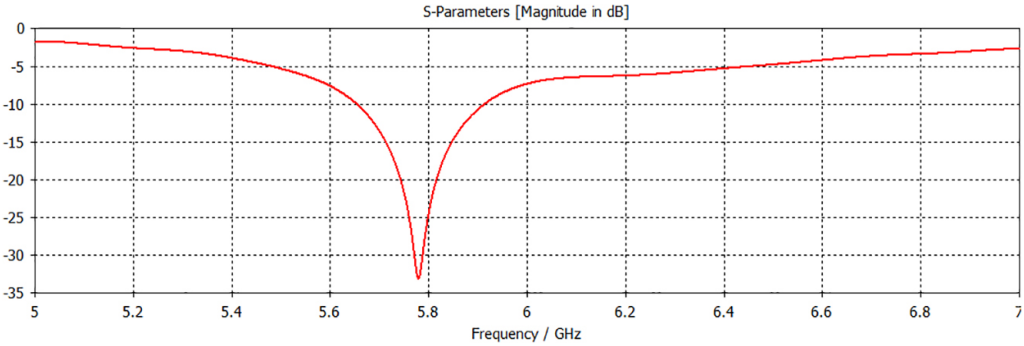


**Fig. 3.** Return loss ($S_{11}$) of the microstrip Bow-Tie antenna

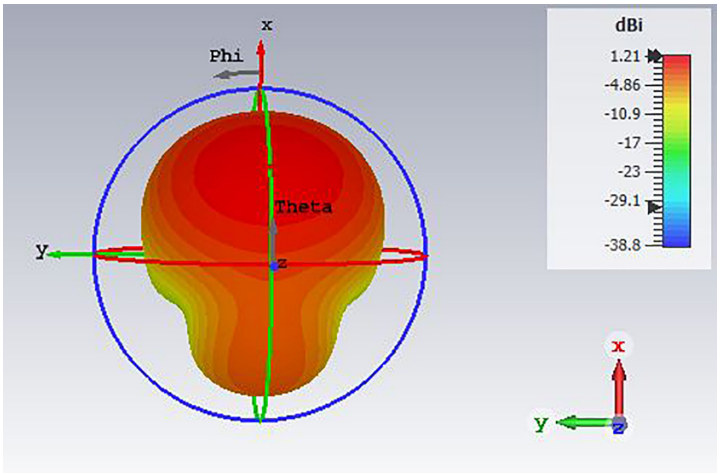


**Fig. 4.** 3D plot of the far-field gain of the microstrip Bow-Tie antenna at a frequency of 5.8 GHz

The 4 × 1 Bow-Tie Patch antenna array was chosen for simulation with the excitation of all four ports simultaneously. The results of this simulation were obtained using CST Studio. As observed in Figures 5 and 6, the return loss at 5.8 GHz is –22.03 dB, and the gain is 3.93 dB.

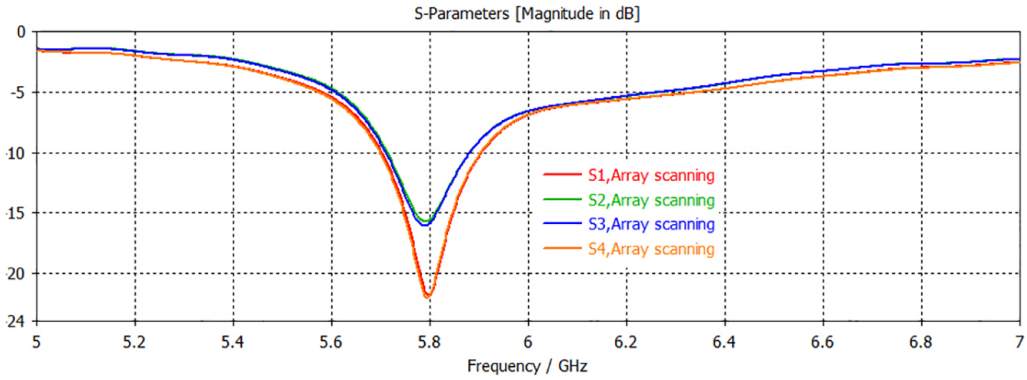


**Fig. 5.** Return loss of the 4 × 1 Bow-Tie antenna array at frequency f = 5.8 GHz with simultaneous excitation, showing the performance for different array scanning configurations (S1, S2, S3, S4)

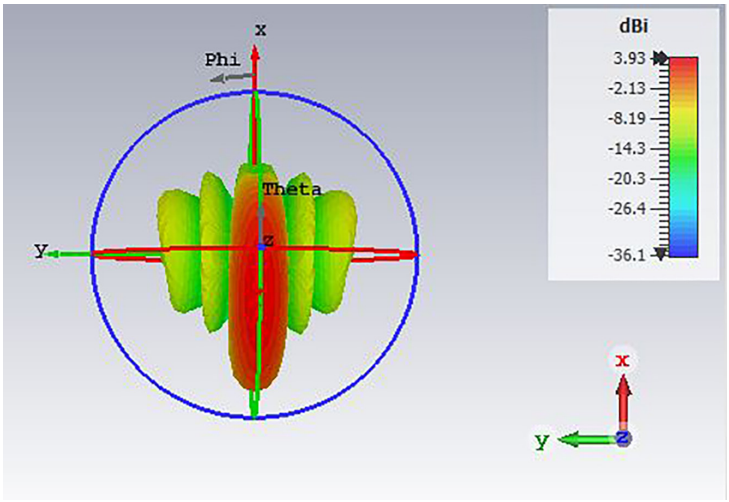


**Fig. 6.** 3D plot of far field gain of microstrip 4 × 1 Bow-Tie antenna array at frequency f = 5.8 GHz with the simultaneous excitation technique

With the four-port simultaneous excitation technique, an enhancement of the return loss value and the gain has been obtained, but not as good as the enhancement we want to reach. A solution that makes the 4 × 1 Bow-Tie Patch antenna array resonate at 5.8 GHz with a better gain and return loss value is to replace the four-port simultaneous excitation technique with the tapered line feeding technique. With the use of this technique of feeding, the design of the 4 × 1 Bow-Tie Patch antenna array is modified as shown in Figure 7.

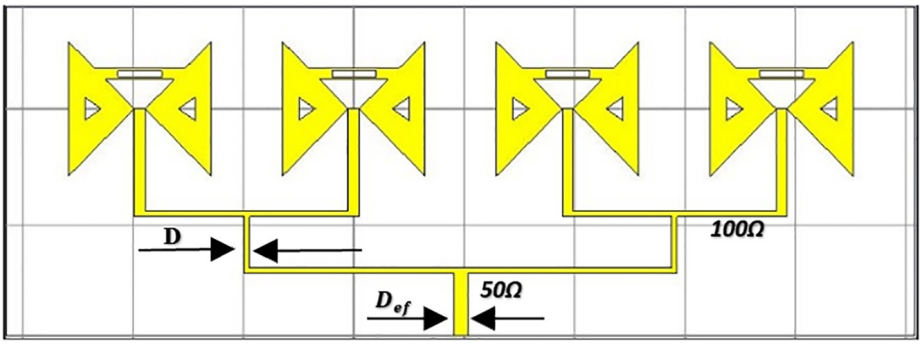


**Fig. 7.** Geometry of the Bow-Tie 4 × 1 Patch antenna array design with tapered line feeding technique, illustrating the impedance matching (50 Ω and 100 Ω lines) and the array configuration

In tapered line technique, the end feeder should be a 50-ohm line, while the other ones should be a 100-ohm line.

To calculate D and $D_{ef}$, we use the transmission line feed width equation which is:

$$D_{ef} = \left\langle \frac{377}{z_0 \sqrt{\varepsilon_r}} \right\rangle h \quad (5) \text{ [33]}$$

$z_0$ = input impedance which is 100-ohm if we calculate D and 50-ohm if we calculate $D_{ef}$, h = height of substrate, $\varepsilon_r$ = permittivity of substrate.

The values of D and $D_{ef}$ obtained with the use of this equation are:

$$D = 1.1 \text{ mm}$$
$$D_{ef} = 2.61 \text{ mm}$$

By comparing the results obtained using the antenna array, the following observations can be made:

- The return loss value increased from –34.45 dB with the single microstrip Bow-Tie antenna to –51.34 dB (see Figure 8) with the 4 × 1 Bow-Tie Patch antenna array.
- The gain value significantly increased from 1.21 dB with the single microstrip Bow-Tie antenna to 11.2 dB (see Figure 9) with the 4 × 1 Bow-Tie Patch antenna array.

These improvements in return loss and gain demonstrate the advantages of using the 4 × 1 Bow-Tie antenna array instead of the single microstrip Bow-Tie antenna. Additionally, with the application of the tapered line technique, it is observed in Figure 8 that the return loss peak reaches –51.34 dB, which is more than twice the value obtained with the previous technique. Furthermore, the gain of the antenna array (see Figure 9) is approximately 11.2 dB, showing a significantly stronger gain compared to the previously obtained value.

Those improvements in return loss and gain values are achieved due to the change in the feeding technique used.

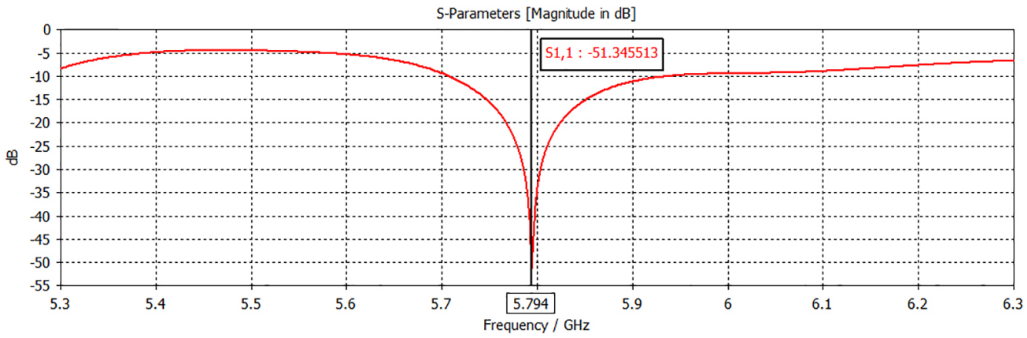


**Fig. 8.** Return loss of the 4 × 1 Bow-Tie antenna array at frequency f = 5.8 GHz with the tapered line feeding technique

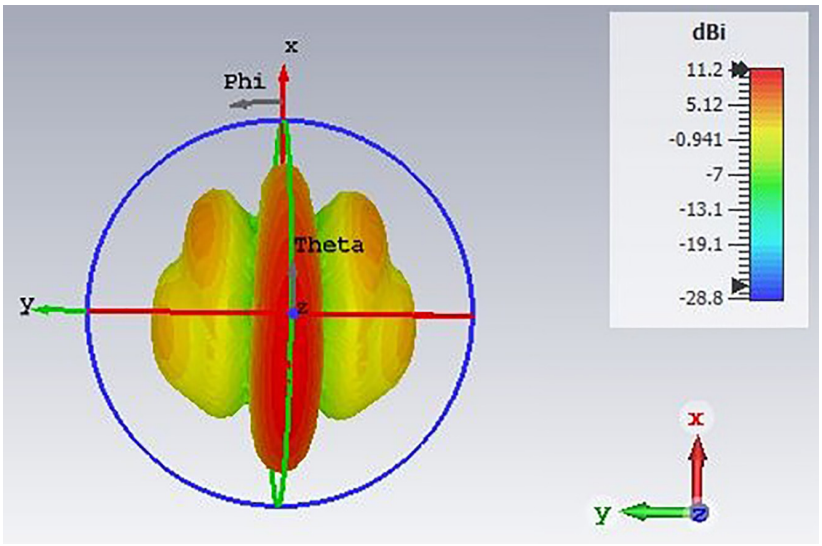


**Fig. 9.** 3D plot of far field gain of microstrip 4 × 1 Bow-Tie antenna array at frequency f = 5.8 GHz with the use of the tapered line feeding technique

Figures 10 and 11 below present photos of the prototypes, showing the dimensions of the single Bow-Tie antenna and the 4 × 1 patch antenna array after fabrication. Both are implemented on an FR4-type substrate with a permittivity of $\varepsilon_r = 4.3$.

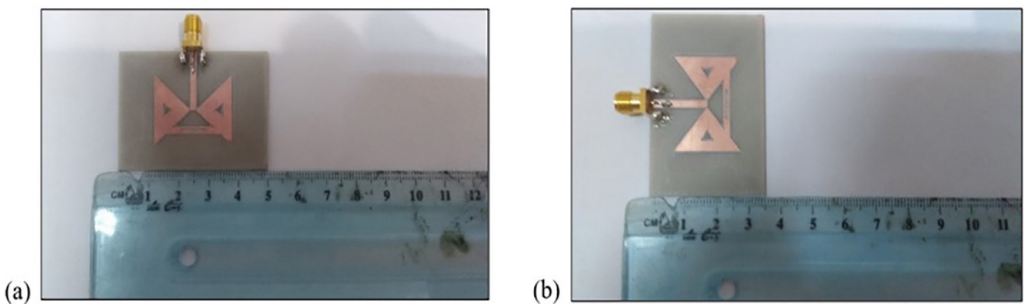


**Fig. 10.** Actual shape and dimensions of the single Bow-Tie Patch antenna: (a) Length measurement of the Bow-Tie Patch antenna; (b) Width measurement of the Bow-Tie Patch antenna array

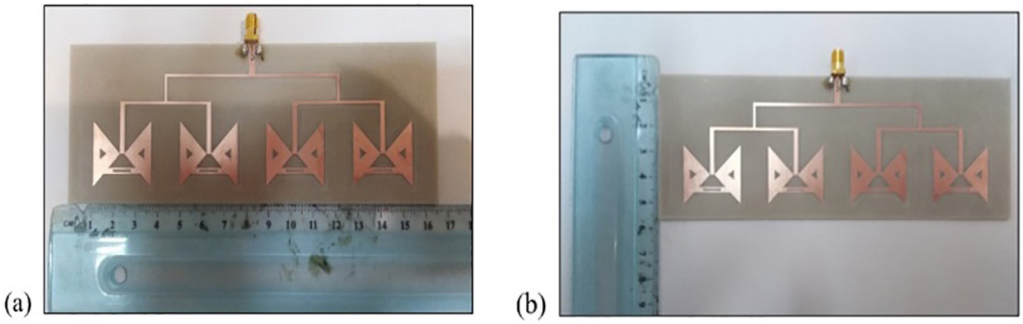

**Fig. 11.** Actual shape and dimensions of the Bow-Tie 4 × 1 Patch antenna array: (a) Length measurement of the Bow-Tie 4 × 1 Patch antenna array; (b) Width measurement of the Bow-Tie 4 × 1 Patch antenna array

Using Copper Mountain Technologies (CMT) network analyzer technology, measurements were conducted on the fabricated microstrip Bow-Tie antenna and the 4 × 1 Bow-Tie Patch antenna array, and the results were obtained as follows:

In Figure 12, the return loss ($S_{11}$) characteristic of the fabricated Bow-Tie antenna is presented. This measurement shows a resonance frequency of 5.82 GHz with a return loss of –41.93 dB. In Figure 13, the return loss ($S_{11}$) characteristic of the fabricated 4 × 1 Bow-Tie patch antenna array is presented. This measurement shows a resonance frequency of 5.81 GHz with a return loss of –44.42 dB.

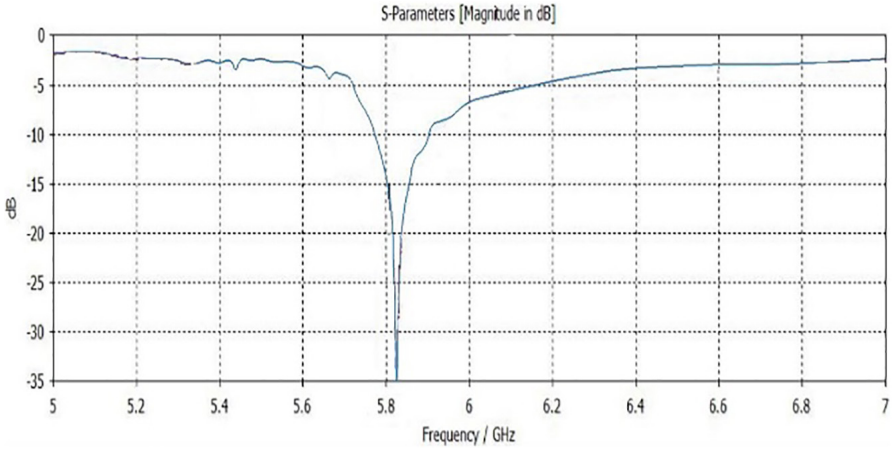


**Fig. 12.** Return loss $S_{11}$ characteristic of the fabricated Bow-Tie antenna

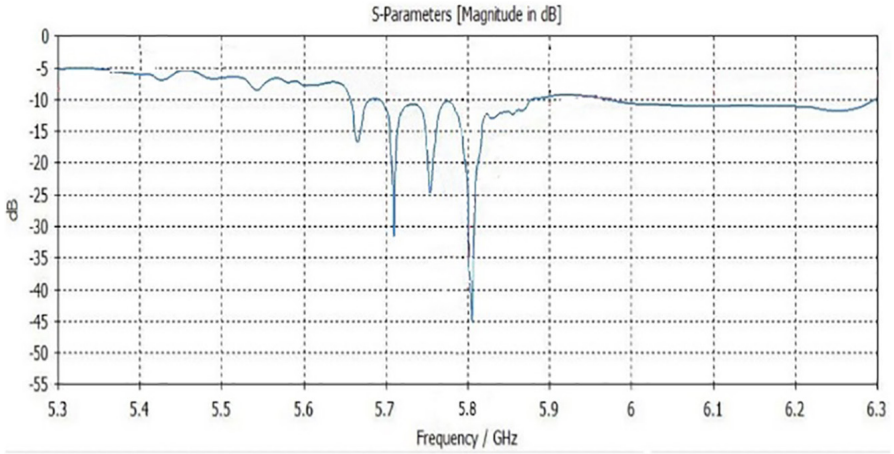


**Fig. 13.** Return loss $S_{11}$ characteristic of the fabricated 4 × 1 Bow-Tie Patch antenna array

In Figure 14 and Table 2, a comparison is presented between the return loss ($S_{11}$) of the fabricated Bow-Tie Patch antenna and that of the simulated Bow-Tie Patch antenna in terms of curve shape and values. For the fabricated antenna, there is excellent concordance between the simulations and measurements over a very wide bandwidth. Specifically, the return loss peak reaches –41.93 dB at 5.82 GHz, which is almost the same value as that obtained with the simulated antenna, occurring at nearly the same frequency of 5.8 GHz.

In Figure 15 and Table 3, a comparison is presented between the return loss ($S_{11}$) of the fabricated 4 × 1 Bow-Tie Patch antenna array and that of the simulated 4 × 1 Bow-Tie Patch antenna array in terms of curve shape and values. Again, excellent concordance is observed between the simulations and measurements over a very wide bandwidth. For the fabricated antenna array, the return loss peak reaches –44.42 dB at 5.81 GHz, compared to –51.34 dB for the simulated antenna, with a slight frequency difference, as the simulated value was obtained at 5.8 GHz.

**Table 2.** $S_{11}$ values of the simulated and fabricated singles antennas according to the frequency

| Frequency/GHz | $S_{11}$/dB Simulated | $S_{11}$/dB Fabricated |
|---|---|---|
| 5 | –1.86 | –1.84 |
| 5.4 | –3.48 | –2.52 |
| 5.6 | –6.79 | –2.61 |
| 5.8 | –34.45 | –41.93 |
| 6 | –7.52 | –7.29 |
| 6.4 | –5 | –2.76 |
| 7 | –2.92 | –2.83 |

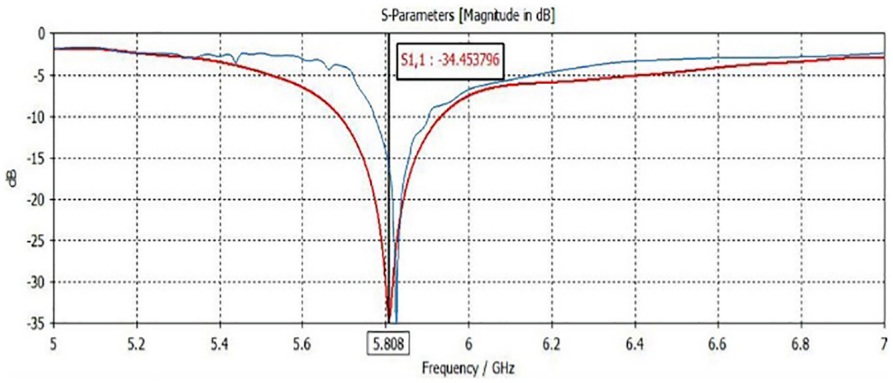


**Fig. 14.** Comparison between the return loss ($S_{11}$) of the fabricated Bow-Tie Patch antenna and the simulated return loss ($S_{11}$) of the Bow-Tie Patch antenna

**Table 3.** $S_{11}$ values of the 4 × 1 simulated and manufactured antennas arrays according to the frequency

| Frequency/GHz | $S_{11}$/dB Simulated | $S_{11}$/dB Fabricated |
|---|---|---|
| 5.3 | –7.92 | –5.03 |
| 5.5 | –4.89 | –6.84 |
| 5.79 | –51.34 | –12.96 |
| 5.81 | –29.23 | –44.42 |
| 6 | –9.95 | 10.67 |
| 6.3 | –6.13 | 9.98 |

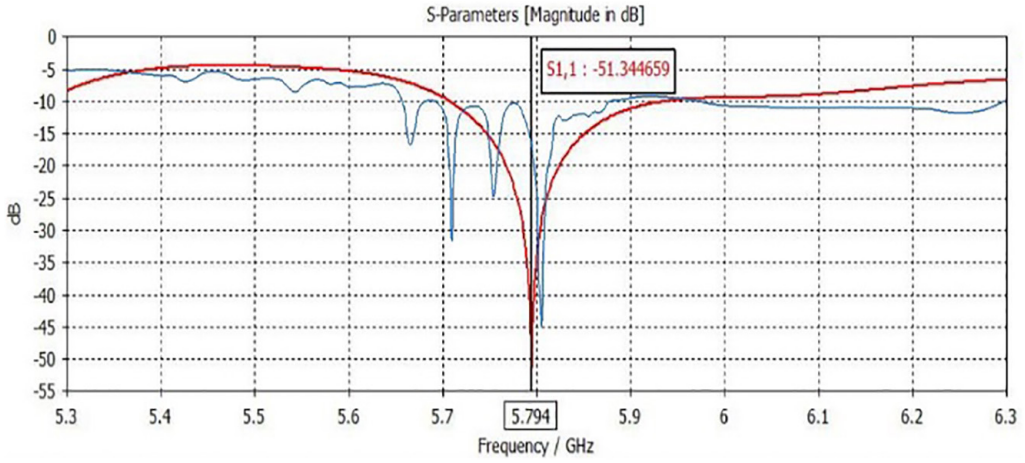


**Fig. 15.** Comparison between the return loss ($S_{11}$) of the fabricated 4 × 1 Bow-Tie Patch antenna array and the return loss ($S_{11}$) of the simulated 4 × 1 Bow-Tie Patch antenna array

**Table 4.** Comparison with other reported antennas

| Ref. | Center Frequency (GHz) | $S_{11}$ Level (dB) | No. of Array Elements | Circuit Size (mm × mm) |
|---|---|---|---|---|
| [34] | 1.06 | 28 | 1 | 17.3 × 17.3 |
| [35] | 7 | 20 | 1 | 30 × 16 |
| [36] | 5.7 | 25 | 1 | 12.8 × 12.8 |
| Proposed antenna | 5.8 | 34.45 | 1 | 30 × 50 |

As shown in Table 4, the comparison table presents various antennas, highlighting attributes such as center frequency, $S_{11}$ level, array elements, and circuit size. The proposed antenna operates at 5.8 GHz, aligning with common healthcare application frequencies and ensuring compatibility with existing standards. Its impressive $S_{11}$ level of –34.45 dB facilitates efficient power transfer, minimizing signal loss and improving overall performance.

With a single array element, the proposed antenna offers simplicity, potentially reducing costs, simplifying manufacturing, and facilitating integration into communication systems. Despite its' slightly larger circuit size of 30 × 50 mm² compared to some competitors, it strikes a balance between performance and space, enabling seamless integration across diverse applications.

Comparing the proposed antenna to referenced designs reveals its competitive edge. For instance, while both the proposed antenna and Ref. 36 operate at similar frequencies, the proposed antenna outperforms Ref. 36 in impedance matching, indicating superior performance. Similarly, compared to Ref. 34, the proposed antenna demonstrates significantly enhanced signal transmission and reception capabilities. Even against Ref. 35, which operates at a higher frequency, the proposed antenna maintains a superior $S_{11}$ level, potentially improving overall performance, particularly in scenarios where signal integrity is critical.

Overall, the proposed antenna exhibits promising compatibility and performance within a suitable frequency spectrum. Its straightforward design enhances its applicability in common healthcare frequencies, although empirical validation remains crucial to confirm its real-world effectiveness.

**Table 5.** Comparison with other reported array of antennas

| Ref. | Center Frequency (GHz) | Matching Level (dB) | No. of Array Elements | Circuit Size (mm × mm) |
|---|---|---|---|---|
| [37] | 5 | 20 | 2 | 47 × 47 |
| [38] | 4 | 22 | 8 | 75 × 150 |
| [39] | 3.66 | 24 | 5 | 30 × 19 |
| [40] | 11.5 | 20 | 8 | 45 × 45 |
| [41] | 1 | 17 | 4 | 30 × 35 |
| [42] | 4.1 | 22 | 4 | 30 × 35 |
| [43] | 2 | 36 | 4 | 30 × 30 |
| Proposed antenna | 5.8 | 51.34 | 4 | 64.5 × 56.5 |

As shown in Table 5, the proposed array antenna operates at a common frequency of 5.8 GHz, ensuring compatibility with wireless communication standards. Its impressive $S_{11}$ level of –51.34 dB indicates efficient power transfer, resulting in minimal signal loss and superior transmission and reception performance.

Featuring four array elements, the antenna strikes a balance between complexity and versatility, enabling beamforming and directional control for various communication scenarios. Despite its' slightly larger circuit size of 64.5 × 56.5 mm$^2$ compared to some antennas, it remains within practical limits for integration.

Comparing the proposed antenna to referenced designs highlights its competitive edge. It significantly outperforms Ref. 33 in matching level, despite operating at similar frequencies. Ref. 34, with a larger array element count, achieves comparable performance, suggesting potential cost savings and design simplicity for the proposed antenna. Against Ref. 36, which operates at a higher frequency, the proposed antenna demonstrates superior signal integrity and efficiency. Similarly, compared to Ref. 39, the proposed antenna exhibits better overall performance, particularly in signal transmission and reception.

In conclusion, the proposed antenna demonstrates exceptional performance, making it an attractive option for communication system integration. However, practical validation remains essential to confirm its real-world effectiveness.

A field-testing scenario for a rural telemedicine deployment could involve setting up the proposed antenna at a remote clinic and linking it to a 5G base station located a few kilometers away or to a satellite backhaul in cases where terrestrial 5G coverage is limited. The primary objective of this trial would be to evaluate the antenna's capability to maintain a stable, high-data-rate connection necessary for applications such as remote ultrasound or the transfer of patient data. Environmental factors such as weather conditions, foliage, and terrain could be evaluated to assess their impact on signal quality. While the 5.8 GHz frequency is less susceptible to heavy rain compared to higher mm wave frequencies, moderate attenuation may still occur, requiring continuous monitoring of link quality to determine the antenna's performance in varying outdoor conditions [44]. Additionally, the presence of local interference, such as from nearby Wi-Fi networks operating within the same frequency band, would be examined. The antenna's directional characteristics could be leveraged to minimize interference from other sources, ensuring that the link remains clean and reliable. This field test would provide valuable insights into the antenna's performance in real-world rural healthcare settings and its potential for supporting critical telemedicine applications [45].

## 4 CONCLUSION

The comparison of the radiation properties of a single Bow-Tie patch antenna with a 4 × 1 Bow-Tie antenna array shows that using the antenna array structure results in better signal strength, range, and quality, along with a return loss value that is superior to that of the single antenna structure at the resonance frequency of 5.8 GHz.

Additionally, an antenna array enables maximum directivity and gain, achieving a high SNR ratio and good performance with minimal power wastage. The use of the tapered line feeding technique instead of the four-port simultaneous excitation technique further increased the return loss peak and improved the gain.

By comparing the results obtained from the CST Microwave Studio software simulations of the antenna and the antenna array with the measurements taken using the CMT network analyzer technology on the fabricated Bow-Tie antenna and the fabricated 4 × 1 Bow-Tie Patch antenna array, it can be concluded that the return loss values of the fabricated antennas align well with the values obtained from the simulations.

## 5 ACKNOWLEDGMENT

The author thanks the Deanship of Scientific Research at Majmaah University for supporting this work.

## 6 REFERENCES

[1] F. Boccardi, R. W. Heath, A. Lozano, T. L. Marzetta, and P. Popovski, "Five disruptive technology directions for 5G," *IEEE Communications Magazine*, vol. 52, no. 2, pp. 74–80, 2014. https://doi.org/10.1109/MCOM.2014.6736746

[2] R. Chávez-Santiago *et al.*, "5G: The convergence of wireless communications," *Wireless Personal Communications*, vol. 83, pp. 1617–1642, 2015. https://doi.org/10.1007/s11277-015-2467-2

[3] D. H. Devi *et al.*, "5G technology in healthcare and wearable devices: A review," *Sensors*, vol. 23, no. 5, p. 2519, 2023. https://doi.org/10.3390/s23052519

[4] H. N. Qureshi, M. Manalastas, A. Ijaz, A. Imran, Y. Liu, and M. O. A. Kalaa, "Communication requirements in 5G-enabled healthcare applications: Review and considerations," *Healthcare*, vol. 10, no. 2, p. 293, 2022. https://doi.org/10.3390/healthcare10020293

[5] A. Kumar, N. Gaur, and A. Nanthaamornphong, "Improving the latency for 5G/B5G based smart healthcare connectivity in rural areas," *Scientific Reports*, vol. 14, p. 6976, 2024. https://doi.org/10.1038/s41598-024-57641-7

[6] V. Agrawal, S. Agrawal, A. Bomanwar, T. Dubey, and A. Jaiswal, "Exploring the risks, benefits, advances, and challenges in internet integration in medicine with the advent of 5G Technology: A Comprehensive Review," *Cureus*, vol. 15, no. 11, 2023. https://doi.org/10.7759/cureus.48767

[7] H. A. Butt, A. Ahad, M. Wasim, F. Madeira, and M. K. Chamran, "5G and IoT for intelligent healthcare: AI and machine learning approaches—A review," in *International Conference on Smart Objects and Technologies for Social Good*, P. J. Coelho, I. M. Pires, and N. V. Lopes, Eds., Springer, Charm, vol. 556, 2023, pp. 107–123. https://doi.org/10.1007/978-3-031-52524-7_8

[8] T.-W. Wang and T.-T. Lin, "Electromagnetic compatibility issues in medical devices," in *Recent Topics in Electromagnetic Compatibility*, IntechOpen, 2022. https://doi.org/10.5772/intechopen.99694

[9] Y. Guo, Y. Feng, and C. Liu, *Antennas and Wireless Power Transfer Methods for Biomedical Applications*. Wiley, 2024. https://doi.org/10.1002/9781119189947

[10] M. J. Iqbal, S. Aurangzeb, M. Aleem, G. Srivastava, and J. C. -W. Lin, "RThreatDroid: A ransomware detection approach to secure IoT based healthcare systems," *IEEE Transactions on Network Science and Engineering*, vol. 10, no. 5, pp. 2574–2583, 2023. https://doi.org/10.1109/TNSE.2022.3188597

[11] H. Elayan, M. Aloqaily, and M. Guizani, "Digital twin for intelligent context-aware IoT healthcare systems," *IEEE Internet of Things Journal*, vol. 8, no. 23, pp. 16749–16757, 2021. https://doi.org/10.1109/JIOT.2021.3051158

[12] R. G. S. Rao and R. Sai, "5G – Introduction & future of mobile broadband communication redefined," *Int. J. Electron. Commun. Instrum. Eng. Res. Dev.*, vol. 3, no. 4, pp. 119–124, 2013.

[13] W. Roh *et al.*, "Millimeter-Wave beamforming as an enabling technology for 5G cellular communications: Theoretical feasibility and prototype results," *IEEE Communications Magazine*, vol. 52, no. 2, pp. 106–113, 2014. https://doi.org/10.1109/MCOM.2014.6736750

[14] P. Pietraski, D. Britz, A. Roy, R. Pragada, and G. Charlton, "Millimeter wave and terahertz communications: Feasibility and challenges," *ZTE Communications*, vol. 10, no. 4, pp. 3–12, 2012.

[15] J. George, M. Deepukumar, C. K. Aanandan, P. Mohanan, and K. G. Nair, "New compact microstrip antenna," *Electronics Letters*, vol. 32, no. 6, pp. 508–509, 1996. https://doi.org/10.1049/el:19960357

[16] M. A. Othman *et al.*, "UWB Bowtie 2 × 2 array antenna for UWB mobile communication system," in *2013 International Conference of Information and Communication Technology (ICoICT)*, 2013, pp. 336–339. https://doi.org/10.1109/ICoICT.2013.6574597

[17] P. J. Soh, M. Mercuri, G. Pandey, G. A. E. Vandenbosch, and D. Schreurs, "Dual-band Planar Bowtie monopole for a fall detection radar and telemetry system," *IEEE Antennas and Wireless Propagation Letters*, vol. 11, pp. 1698–1701, 2012. https://doi.org/10.1109/LAWP.2013.2238501

[18] M. N. A. Karim, M. F. A. Malek, M. F. Jamlos, L. Y. Seng, and N. Saudin, "Design of ground penetrating radar antenna for buried object detection," in *2013 IEEE International RF and Microwave Conference (RFM)*, 2013, pp. 253–257. https://doi.org/10.1109/RFM.2013.6757260

[19] W.-L. Chen, G.-M. Wang, and C.-X. Zhang, "Bandwidth enhancement of a microstrip-line-fed printed wide-slot antenna with a fractal-shaped slot," *IEEE Trans. Antennas Propag.*, vol. 57, no. 7, pp. 2176–2179, 2009. https://doi.org/10.1109/TAP.2009.2021974

[20] C. H. See, R. A. Abd-Alhameed, D. Zhou, T. H. Lee, and P. S. Excell, "A crescent-shaped multiband planar monopole antenna for mobilewireless applications," *IEEE Antennas Wirel. Propag. Lett.*, vol. 9, pp. 152–155, 2010. https://doi.org/10.1109/LAWP.2010.2044741

[21] H. Eskandari, M. R. Booket, M. Kamyab, and M. Veysi, "Investigations on a class of wideband printed slot antenna," *IEEE Antennas Wirel. Propag. Lett.*, vol. 9, pp. 1221–1224, 2010. https://doi.org/10.1109/LAWP.2010.2100360

[22] J. Gosalvitr, C. Mahatthanajatuphat, P. Akkaraekthalin, and S. Chaimool, "CPW-fed slot antenna with fractal tuning stub for wideband circular polarization," in *Proceedings of the 8th Electrical Engineering/Electronics, Computer, Telecommunications and Information Technology (ECTI) Association of Thailand*, 2011, pp. 212–215. https://doi.org/10.1109/ECTICON.2011.5947810

[23] K. Song, Y.-Z. Yin, B. Chen, S. T. Fan, and F. Gao, "Bandwidth enhancement design of compact UWB step-slot antenna with rotated patch," *Prog. Electromagn. Res. Lett.*, vol. 22, pp. 39–45, 2011. https://doi.org/10.2528/PIERL11030112

[24] C. Tze-Hsuan and K. Jean-Fu, "Compact multi-band h-shaped slot antenna," *IEEE Trans. Antennas Propag.*, vol. 61, no. 8, pp. 4345–4349, 2013. https://doi.org/10.1109/TAP.2013.2262666

[25] Q. L. Zhang, L.-M. Si, Y. M. Wu, Y. Liu, and X. Lv, "Design of a coplanar bowtie antenna for WLAN and WiMAX application," in *Proceedings of the 3rd Asia-Pacific Conference on Antennas and Propagation*, 2014, pp. 284–286. https://doi.org/10.1109/APCAP.2014.6992475

[26] S. Mukherjee, A. Biswas, and K. V. Srivastav, "Substrate integrated waveguide cavity backed slot antenna with parasitic slots for dual-frequency and broadband application," in *2014 44th European Microwave Conference*, 2014, pp. 57–60. https://doi.org/10.1109/EuMC.2014.6986368

[27] A. Alsaraira, O. A. Saraereh, and S. Alabed, "Advancements in breast cancer detection through broadband microstrip antenna technology," *International Journal of Online and Biomedical Engineering (iJOE)*, vol. 20, no. 13, pp. 41–59, 2024. https://doi.org/10.3991/ijoe.v20i13.50509

[28] S. Rana, J. Verma, and A. K. Gautam, "Design and analysis of wideband stair step-shaped rectangular ring microstrip antenna with DGS for IoT applications," *International Journal of Online and Biomedical Engineering (iJOE)*, vol. 19, no. 9, pp. 122–130, 2023. https://doi.org/10.3991/ijoe.v19i09.37065

[29] M. A. Shaikh, M. A. Khuhro, S. A. Shaikh, and K. K. Khatri, "Cost-effective electromagnetic lens-assisted microstrip patch antenna design for location-based services in 5G/6G technology radio frequency front end," *International Journal of Online and Biomedical Engineering (iJOE)*, vo. 21, no. 1, pp. 165–175, 2025. https://doi.org/10.3991/ijoe.v21i01.53035

[30] yu-De Lin and Syh-Nan Tsai, "Coplanar waveguide-fed uniplanar bow-tie antenna," *IEEE Tras .on antennas and propagations*, vol. 45, no. 2, pp. 305–306, 1997. https://doi.org/10.1109/8.560350

[31] Z. Guiping, A. A. Kishk, A. B. Yakolev and A. W. Glissan, "A Broadband printed bow-tie antenna with a similar feed," *IEEE*, vol. 4, 1984.

[32] S. Sadek and Z. Katbay, "Ultra-wideband CPW Bowtie antenna," in *International Conference on Electromagnetics in Advanced Applications*, 2009, pp. 261–263. https://doi.org/10.1109/ICEAA.2009.5297451

[33] K. P. Yang and K. L. Wong, "Dual band circularly polarized square microstrip antenna," *IEEE Trans. Antennas Propagate.*, vol. 49, no. 3, pp. 377–382, 2001. https://doi.org/10.1109/8.918611

[34] A. Hocini, N. Melouki, and T. Denidni, "Modeling and simulation of an antenna with optimized AMC reflecting layer for gain and front-to-back ratio enhancement for 5G applications," *J. Phys. Conf. Ser.*, vol. 1492, no. 1, p. 12006, 2020. https://doi.org/10.1088/1742-6596/1492/1/012006

[35] A. Althuwayb, "MTM-and SIW-inspired bowtie antenna loaded with AMC for 5G mm-wave applications," *Int. J. Antennas Propa.*, vol. 2021, no. 1, p 6658819, 2021. https://doi.org/10.1155/2021/6658819

[36] W. Wan, M. Xue, L. Cao, T. Ye, and Q. Wang, "Wideband low-profile AMC-based patch antenna for 5G antenna-in-package application," in *Proceedings of the 2020 IEEE 70th Electronic Components and Technology Conference (ECTC)*, 2020, pp. 1818–1823. https://doi.org/10.1109/ECTC32862.2020.00284

[37] A. Ibrahima and W. Ali, "High gain, wideband and low mutual coupling AMC-based millimeter wave MIMO antenna for 5G NR networks," *AEU Int. J. Electron. Commun.*, vol. 142, p. 153990, 2021. https://doi.org/10.1016/j.aeue.2021.153990

[38] N. Parchin, R. Abd-Alhameed, Y. Li, M. Nielsen, and M. Shen, "High-performance Yagi-Uda antenna array for 28 GHz mobile communications," in *Proceedings of the 27th Telecomm Forum TELFOR*, 2019, pp. 1–4. https://doi.org/10.1109/TELFOR48224.2019.8971142

[39] J. Nasir, M. Rehman, A. Hashmi, and W. A. Khan, "Compact low-cost high isolation substrate integrated waveguide fed slot antenna array at 28 GHz employing Beamforming and Beam Scanning for 5G Applications," in *Proceedings of the 12th European Conference on Antennas and Propagation (EuCAP 2018)*, 2018, pp. 1–5. https://doi.org/10.1049/cp.2018.1202

[40] S. Ta, H. Choo, and I. Park, "Broadband printed-dipole antenna, and its arrays for 5G applications," *IEEE Antennas Wirel. Propag. Lett.*, vol. 16, pp. 2183–2186, 2017. https://doi.org/10.1109/LAWP.2017.2703850

[41] M. Bilal, S. I. Naqvi, N. Hussain, Y. Amin, and N. Kim, "High-isolation MIMO antenna for 5G millimeter-wave communication systems," *Electronics,* vol. 11, no. 6, p. 962, 2022. https://doi.org/10.3390/electronics11060962

[42] M. Khalid *et al.*, "4-Port MIMO antenna with defected ground structure for 5G millimeter wave applications," *Electronics,* vol. 9, no. 1, p. 71, 2020. https://doi.org/10.3390/electronics9010071

[43] M. M. Kamal *et al.*, "Infinity shell shaped MIMOAntenna array for mm-wave 5G applications," *Electronics,* vol. 10, no. 2, p. 165, 2021. https://doi.org/10.3390/electronics10020165

[44] Y. Zhang, D. J. Love, J. V. Krogmeier, C. R. Anderson, R. W. Heath, and D. R. Buckmaster, "Challenges and opportunities of future rural wireless communications," *IEEE Communications Magazine*, vol. 59, no. 12, pp. 16–22, 2021. https://doi.org/10.1109/MCOM.001.2100280

[45] S. Wu *et al.*, "Pilot study of robot-assisted teleultrasound based on 5G network: A new feasible strategy for early imaging assessment during COVID-19 pandemic," *IEEE Transactions on Ultrasonics, Ferroelectrics, and Frequency Control,* vol. 67, no. 11, pp. 2241–2248, 2020. https://doi.org/10.1109/TUFFC.2020.3020721

## 7 AUTHORS

**Zribi Chedly** is a PhD student in Electronics, focusing on the design of graphene-based antennas for 5G applications. He holds a master's degree in Electronics, Electrotechnics, and Automation, which he obtained in 2020 from the Faculty of Sciences of Tunis. Currently, he is conducting his study at the High-Frequency Electronics Research Laboratory. His work primarily explores the use of graphene to improve antenna performance for next-generation communication technologies.

**Beldi Sabri** received the master's degree in electrical engineering from the Faculty of Sciences of Tunis, Tunisia. He received his PhD in Electronics in 2016 from the Faculty of Sciences of Tunis, Tunisia. And was named an assistant professor of Electrical Engineering in 2016. His main scientific interests cover investigation of planar passive elements and subsystems of microwave technology, propagation of electromagnetic waves in periodic structures and metamaterials. He is the author or coauthor of more than 25 publications in scientific journals, including international ones as well as national conferences.

**Prof. Azizi Mohamed Karim** received the master's degree in Telecommunications from Supcom, Tunisia in 2008, and Ph.D. degree in Electronics from Faculty of Sciences of Tunis, Tunisia in 2013. He is currently an Associate Professor in electronics at Higher Institute of Multimedias Arts of Manouba, University of Manouba, Tunisia. Where he has been teaching since 2009. Presently, he is the Director of Internships and he's in Charge of Video Game Development Program at Higher Institute of Multimedias Arts of Manouba.

**Amor Smida** (Member, IEEE) received the degree in electronic baccalaureate and the M.Sc. degree in analysis and digital processing of electronic systems, in 2008 and

2010, respectively, and the Ph.D. degree from the Faculty of Mathematical, Physical and Natural Sciences of Tunis, University of Tunis El Manar, Tunisia, in 2014. From 2008 to 2014, he was a Graduate Student Researcher with the Unit of Research in High Frequency Electronic Circuits and Systems. Since August 2014, he has been an Assistant Professor with the Department of Medical Equipment Technology, College of Applied Medical Sciences, Majmaah University, Saudi Arabia. His current research interests include smart antennas and biosensors.

**Naif Hadeed Al-Mutairi** obtained a bachelor's degree in Medical Equipment Technology from Majmaah University in 2018 and a master's degree in biomedical engineering from Majmaah University in 2022. He currently works as a Senior Specialist at King Khalid Hospital in Al-Majmaah.

**Mohamed Ibrahim Waly** received the degree in biomedical engineering and system baccalaureate, the M.Sc. degree in biomedical engineering and systems, and the Ph.D. degree from the Faculty of Biomedical Engineering and Systems, Cairo University, in 2004, 2009, and 2013, respectively. From 2004 to 2015 and from 2013 to 2015, he was a Consultant Engineer with CASBEC. Since September 2022, he has been an Associate Professor with the Department of Medical Equipment Technology, College of Applied Medical Sciences, Majmaah University, Saudi Arabia. His current research interests include design microwave antennas for biomedical applications, machine learning applications in the medical field, prediction disease models, system dynamic models, and clinical engineering management systems (E-mail: m.waly@mu.edu.sa).